WATER RESOURCES RESEARCH, VOL. 32, NO. 6, PAGES 1585–1595, JUNE 1996

Stochastic analysis of solute transport in heterogeneous, variably saturated soils

Thomas Harter

Department of Land, Air, and Water Resources, University of California, Davis

T.-C. Jim Yeh

Department of Hydrology and Water Resources, University of Arizona, Tucson

Abstract. Statistical moments of solute plumes from small sources in variably saturated, heterogeneous porous media are analyzed by using a newly developed, efficient high-resolution Monte Carlo technique. In agreement with previous theoretical work, it is illustrated that the prediction of such solute plumes is associated with large uncertainties for dimensionless travel times, t', exceeding 40, particularly predictions of plumes in highly heterogeneous soils ($\sigma_y^2 > 2$). Uncertainty about the travel path of the plume center contributes significantly to overall concentration uncertainty as flux fields become more variable. It is shown that the concentration coefficient of variation at the center of the plume initially increases but stagnates or decreases at later times. For highly heterogeneous soil flux conditions or for the common case of soils with strongly anisotropic conditions, analytical models underestimate transverse spreading of the mean concentration plume at any given time, while overestimating longitudinal spreading. At identical mean plume displacement distances, analytical models underestimate both transverse and longitudinal spreading and overestimate the variance of solute flux (breakthrough curve) by up to a factor 4. As an alternative to the statistical analysis of solute flux, we propose to analyze statistical properties of time associated with peak solute flux and with first exceedance of a given solute flux level.

Introduction

Most groundwater pollution sources, whether they are agricultural, domestic, or industrial, are generally at or near the surface, and pollutants must travel through the unsaturated zone before reaching groundwater. Thus a thorough understanding of transport processes in the unsaturated zone is essential to assess the contamination risk of groundwater resources and to predict travel time from a pollution source to a drinking water well field. Stochastic models of solute transport in variably saturated media that account for uncertainty due to spatial variability have mostly been limited to the analysis of one-dimensional scenarios [e.g., *Dagan and Bresler*, 1979; *Bresler and Dagan*, 1981; *Amoozegar-Fard et al*., 1982; *Jury*, 1982; *Simmons*, 1982; *Jury et al*., 1986; *Butters and Jury*, 1989; *Destouni and Cvetkovic*, 1989, 1991]. These studies assume that soils consist of an ensemble of independent, random, vertically homogeneous stream tubes and that horizontal movement of solutes is negligible.

Two-dimensional solute transport in heterogeneous soils under unsaturated conditions has recently been studied numerically by *Russo* [1991] and by *Russo and Dagan* [1991] who suggested that macrodispersion of unsaturated transport is amenable to the same stochastic transport analysis as those known for aquifer contamination. *Russo* [1993a] combined the three-dimensional spectral analysis of unsaturated flow in heterogeneous media by *Yeh et al*. [1985a, b] with the Lagrangian transport analysis by *Dagan* [1988] to derive analytical expressions for the displacement of the center of a plume and for the average plume spreading. In a complementary study, *Russo* [1993b] derived the mean solute breakthrough in a three-dimensionally heterogeneous soil based on the work by *Cvetkovic et al*. [1992]. These analyses are accurate only to first order and thus restricted to mildly heterogeneous media with a normally distributed velocity. As demonstrated in many field and theoretical studies [e.g., *Yeh et al*., 1985b, c, 1986; *Yeh and Harvey*, 1990], variability in unsaturated hydraulic properties can become large as soil desaturates, indicating that variability of flux under relatively dry conditions can be very strong. In addition, *Harter* [1994] demonstrated that vertical Darcy flux distribution is skewed, which contrasts with the Gaussian flux distribution assumed in analytical studies. Clearly, the validity of analytical macrodispersion models needs to be assessed.

The purpose of this paper is to implement high-resolution Monte Carlo simulations (MCS) to improve our understanding of solute transport in highly heterogeneous systems and to compare results with existing analytical models. We focus on the behavior of solute plumes from point sources and investigate solute concentration, solute flux, and solute plume spreading as a function of the various independent parameters characterizing a spatially variable soil. Concentration moments and solute plume spreading are analyzed and compared to a linear macrodispersion model similar to that of *Dagan* [1988]. Solute flux and travel time in various soils are investigated and compared to the Lagrangian particle travel time model by *Cvetkovic et al*. [1992].

Paper number 96WR00502.
0043-1397/96/96WR-00502$09.00

Implementation of Monte Carlo Simulation

Transport Model

Transient transport is simulated with an algorithm by *Yeh et al*. [1993] based on the modified method of characteristics (MMOC). Given a random realization $\mathbf{v}(\mathbf{x})$ of the velocity field and a local dispersion tensor $\mathbf{D}(\mathbf{x})$, the governing equation for concentration $c(\mathbf{x}, t)$ solved by MMOC is

$$\frac{\partial c(\mathbf{x}, t)}{\partial t} + \mathbf{v}(\mathbf{x})\nabla c(\mathbf{x}, t) = \nabla \cdot [\mathbf{D}(\mathbf{x})\nabla c(\mathbf{x}, t)] \qquad (1)$$

Detailed methods for generating random realizations of steady state, unsaturated velocity fields $\mathbf{v}(\mathbf{x})$ are given by *Harter* [1994]. Input parameters are mean soil water tension H and spatially correlated random realizations of f (logarithm of the saturated hydraulic conductivity: $f = \ln K_s$) and a (logarithm of the pore size distribution parameter: $a = \ln \alpha$) with means F and A, and variance σ_f^2 and σ_a^2, respectively, and an exponential spatial correlation function characterized by the horizontal and vertical correlation scales λ_{fx} and λ_{fz}. The correlation function for a is assumed identical to that of f.

In this study, $\mathbf{D}$ is set to 0, which allows for a numerically efficient implementation of (1). Local or "pore-scale" dispersion is introduced implicitly through numerical dispersion, which is caused by the bilinear interpolation scheme employed in the advective step of the MMOC [*Yeh et al*., 1993]. Its actual magnitude is determined as part of this study. Implicit (numerical) or explicit (parametric) local dispersion is expected to affect local concentration variance [*Dagan*, 1982] and the asymptotic (i.e., late time) magnitude of lateral macrodispersion [*Gelhar and Axness*, 1983; *Neuman et al*., 1987]. While numerical dispersion is artificial, its net effect is consistent with many field findings and with the stochastic transport theories of *Gelhar and Axness* [1983], and *Neuman et al*. [1987], which explicitly account for pore-scale dispersion.

Statistical Analysis of Monte Carlo Simulations

Spatial concentration distribution. In this analysis the local concentration sample mean $\langle c(\mathbf{x}, t)\rangle$ and the local sample variance $\sigma_c^2(\mathbf{x}, t)$ are evaluated at four dimensionless times, $t' = 5$, 10, 20, and 40 (at one site the output is compiled at times $t' = 4$, 8, 16, and 31), where $t' = t\, V_z^{\text{num}}/\lambda_{fz}$, with V_z^{num} being the actual vertical mean velocity determined from MCS. The zero-order, first-order, and second-order spatial moments of an actual concentration plume are given as

$$M_0(t) = \sum_{i=1}^{NN} c(\mathbf{x}^i, t)\theta(\mathbf{x}^i)\Delta x^i \Delta z^i$$

$$M_x(t) = 1/M_0 \sum_{i=1}^{NN} c(\mathbf{x}^i, t)\theta(\mathbf{x}^i)\Delta x^i \Delta z^i x^i$$

$$M_z(t) = 1/M_0 \sum_{i=1}^{NN} c(\mathbf{x}^i, t)\theta(\mathbf{x}^i)\Delta x^i \Delta z^i z^i \qquad (2)$$

$$M_{xx}(t) = \left[1/M_0 \sum_{i=1}^{NN} c(\mathbf{x}^i, t)\theta(\mathbf{x}^i)\Delta x^i \Delta z^i (x^i)^2 \right] - (M_x(t))^2$$

$$M_{zz}(t) = \left[1/M_0 \sum_{i=1}^{NN} c(\mathbf{x}^i, t)\theta(\mathbf{x}^i)\Delta x^i \Delta z^i (z^i)^2 \right] - (M_z(t))^2$$

$M_0(t)$ is total mass in the finite element domain, where the finite element domain consists of NN nodes connecting rectangular elements of sidelengths Δx and Δz. $\theta(\mathbf{x}^i)$ is the arithmetic average of water content in the four elements surrounding node I. In this study, θ is assumed constant throughout the domain, consistent with existing analytical models against which we will compare our results. The horizontal and vertical positions, $M_x(t)$ and $M_z(t)$, are the center of mass of a plume $c(\mathbf{x}, t)$, $\mathbf{x} \in \mathbb{R}^2$. The terms $M_{xx}(t)$ and $M_{zz}(t)$ are horizontal and vertical moments of inertia, respectively. From realizations of random, time-dependent moments (2), sample means and sample variances are computed at 500 equally distant time intervals distributed over the total simulation period.

The variance of $M_0(t)$ is an indicator of the average numerical mass balance error in MMOC. The expected values of the first spatial moments, $\langle M_x(t)\rangle$ and $\langle M_z(t)\rangle$, are measures of average plume displacement and coincide with the center of mass of the mean plume concentration $\langle c(\mathbf{x})\rangle$. The mean of the second spatial moment $\langle M_{ii}(t)\rangle$ $(I = x, z)$ is a representative measure of the average spreading of the plume around its centroid. Second spatial moments, $\langle M_{ii}(t)\rangle$, are not identical to second moments, $X_{ii}(t)$, of the mean concentration plume [cf. *Dagan*, 1990]. The first and second spatial moment X_i and X_{ii} of the mean concentration plume $\langle c(\mathbf{x}, t)\rangle$ are computed as in (2), with $c(\mathbf{x}, t)$ replaced by $\langle c(\mathbf{x}, t)\rangle$ and M replaced by X. From statistical principles for turbulent mixing [*Fischer et al*., 1979], illustrated by *Kitanidis* [1988] and *Dagan* [1990] for porous media transport, it follows that X_{ii}, $\langle M_{ii}\rangle$, and var (M_i) are related through

$$\langle M_{ii}(t)\rangle + \text{var}\,[M_i(t)] = X_{ii}(t) \qquad i = x, z \qquad (3)$$

where var (M_i) is the sample variance of the first spatial moment M_i, that is, it is a measure of the uncertainty regarding the actual center of a solute plume. Uncertainty about the travel path of the plume center, var (M_i), relative to the size of $\langle M_{ii}\rangle$ vanishes only if plumes are of large initial lateral spreading or have traveled a sufficiently large distance. Then $\langle M_{ii}\rangle$ and X_{ii} become interchangeable (ergodic transport).

Solute flux characteristics. In applications to the unsaturated zone, solute mass flux across a compliance boundary (usually the water table) is of significant practical interest. Neglecting pore-scale dispersion, solute flux $s(\mathbf{x}, t)$, the mass of solute per unit area and unit time passing through a surface element of unit normal η is related to the resident concentration $c(\mathbf{x}, t)$:

$$s(\mathbf{x}, t) = \mathbf{s}(\mathbf{x}, t) \cdot \eta = c(\mathbf{x}, t)\theta_e \mathbf{v}(\mathbf{x}) \cdot \eta \qquad (4)$$

Definition (4) yields a flux-averaged concentration, $c_q = \int (\mathbf{s}\ \eta\ dA)/\int (\theta_e \mathbf{v} \eta\ dA)$, equal to resident concentration. Such a simplification is justified because advective mass flux here is much larger than dispersive mass flux [*Parker and Van Genuchten*, 1984].

Total mass flux $S(t)$ across a compliance surface (CS), here a single line perpendicular to the mean flow direction, is

$$S(t) = \sum_{n=1}^{NC} s(\mathbf{x}_i, t)\Delta x_i \qquad (5)$$

NC is the number of finite element nodes along the horizontal CS, and Δx_i is the average element width to the left and right of node I; in other words, concentration is linearly weighted between nodes. Mean $\langle S(t)\rangle$ and variance $\sigma_s^2(t)$ of $S(t)$ are

computed from individual realizations of the integrated mass breakthrough curves $S(t)$. For this study, four CS's are defined at dimensionless vertical distances $Z' = Z/\lambda_{fz} = 5.4$, 11.6, 17.8, and 23.8 from the solute source area.

In addition to the stochastic analysis of total mass breakthrough $S(t)$, a stochastic analysis of solute mass flux arrival time $t_a(\mathbf{x}, s)$, and solute peak flux time $t_p(\mathbf{x})$ is undertaken. Solute mass flux arrival $t_a(\mathbf{x}, s)$ is the time at which solute mass flux first exceeds a compliance mass flux s at location $\mathbf{x}$ on the CS. Mean, $\langle t_a(\mathbf{x}, s)\rangle$, and variance, var $t_a(\mathbf{x}, s)$, are computed at 19 discrete levels s distributed logarithmically between $10^{-9} \times s/s_0$ and $10^{-0.5} \times s/s_0$. Peak flux time $t_p(\mathbf{x})$ is equal to time of highest concentration or peak solute flux at $\mathbf{x}$. Statistical moments of arrival and peak time are investigated at one horizontal compliance surface near the center of the simulation domain ($Z' = 11.6$). Results are normalized with respect to spatially invariable water content θ and mean vertical velocity $V_{\text{num},z}$.

Model Soil Sites

Numerical simulations are implemented for soil cross sections that are 12.8 m deep and between 7.6 and 30 m wide, depending on the expected horizontal solute spreading. Our model simulates instantaneous injection of a small source solute slug into soils by specifying an initial concentration $c_0 = 1$ for a rectangle of three nodes horizontally by two nodes vertically (concentration is specified as a nodal property in MMOC). Total applied mass depends on grid discretization. Reported sample moments are normalized with respect to total mass or initial concentration. They depend only on the ratio between initial plume size and correlation scale of the saturated hydraulic conductivity.

Hypothetical soil types are investigated that are representative of a wide variety of typical field soils. All soils have a hypothetical vertical correlation length $\lambda_{fz} = 0.5$ m. The horizontal correlation length λ_{fx} varies from 0.5 to 3.0 m. Vertical discretization of the finite element domain is 0.1 m. Horizontal discretization is 0.1 m for $\lambda_{fx} = 0.5$ m, 0.15 m for $\lambda_{fx} = 1.5$ m, and 0.3 m for $\lambda_{fx} = 3.0$ m. Thus the size of the initial solute slug is 0.4 λ_{fz} by 0.6 λ_{fx} for isotropic soils, and 0.4 λ_{fz} by 0.3 λ_{fx} for anisotropic soils. Total size of the finite element domain is 128 elements vertically and between 76 and 100 elements horizontally. Horizontal domain size was chosen such that solute plumes would not be affected by the vertical boundaries of the finite element domain. The variance of f varies from 0.01 to 3.6, and the variance of a from 0.0001 to 0.04. The correlation ρ_{af} between f and a is either 1 or 0. The geometric mean of α (=Γ) is always 1.0 m^{-1}. The average water tension H varies from -1.5 to -30 m. A parameter summary of the different hypothetical soils is given in Table 1 together with the actual size and discretization of the respective flow and transport models. For easier reference, soils are grouped into four different categories that address the sensitivity of stochastic transport to specific parameters:

1. Isotropic, wet soil; soils 2, 8, 3, and 9. Only the variances of f and a change. The resulting average sample variance σ_y^2 of the logarithm of the unsaturated hydraulic conductivity $y = \log K$ is 0.01, 0.12, 0.85, and 3.4. Mean pressure head for "wet" soils is -1.50 m.

2. Anisotropic, wet soil; soils 12, 29, 28, 22. Again, only the variance of f and a change. For soils 29, 28, and 22 the resulting variance of y is 0.74, 1.8, and 3.2; soils 12 and 29 have identical variances in f and a, but unlike all other examples, soil 12 has perfectly correlated f and a random fields, which reduces the unsaturated hydraulic conductivity variance to 0.53.

3. Constant variance $\sigma_f^2 = 1$, wet soil; soils 3, 31, 29. Only the horizontal correlation scale of f (and a) change: For the three soils they are 0.5, 1.5, and 3.0 m, which results in aspect ratios $\nu = \lambda_{fx}/\lambda_{fz} = 1$, 3, and 6, respectively. The three soils have similar σ_y^2: 0.85, 0.79, and 0.74.

4. Anisotropic dry soil; soils 15 and 21. These are both dry soils with mean soil water tensions H of -10.0 and -30.0 m, respectively. Apart from differences in pressure head, soil 15 is identical to soil 29, and soil 21 is identical to 12. The two dry soils are compared with two strongly heterogeneous wet soils of similar unsaturated hydraulic conductivity variance: 15 is compared with 28 ($\sigma_y^2 = 1.5$ and 1.8, respectively), 21 is compared with 22 ($\sigma_y^2 = 3.2$ for both).

In the remainder of the paper, soil sites are referred to by their category name and the value of σ_y^2. *Harter* [1994] showed that σ_y^2 is the most important indicator for the heterogeneity of the velocity field and is expected to play a similar role for describing heterogeneity of solute concentration and flux.

To avoid errors due to first-order random head boundary, the transport equation is solved in a different finite element grid than the flow simulation. Steady state flux is obtained for a finite element domain that is 5 to 10 elements larger around each side than the finite element domain for the transport simulation. In other words, boundaries of the transport model are located in the interior of the flow model. The size of the peripheral "cutoff" within the flow model is determined from the MCS of unsaturated flow [*Harter*, 1994] and is indicated in the right column of Table 1.

Monte Carlo simulations are based on 300 realizations of each soil site. The accuracy of the sample mean concentrations calculated from 300 realizations and the rate of convergence in the MCS was investigated by *Harter* [1994]. Mean concentrations at different travel times computed from 100, 300, and 1000 realizations were compared, and it was found that mean concentrations based on 1000 realizations do not significantly differ from those based on 300 realizations. Experiments with 300 realizations gave significantly smoother mean concentration contours than contour maps based on 100 realizations,

Table 1. Input Parameters for the Various Hypothetical Soil Sites Used in the Unconditional Transport Analysis

Soil Site	σ_f^2	σ_s^2	ρ	Γ	H	Δx	λ_{fx}	Cut
3	0.95	0.01	0	1.0	−1.5	0.1	0.5	5
2	0.01	10^{-4}	···	···	···	···	···	2
4	···	···	1	···	···	···	···	5
8	0.12	···	···	···	···	···	···	5
9	3.6	0.04	···	···	···	···	···	10
12	···	···	1	···	···	0.3	3.0	5
15	···	···	···	···	−10.0	0.3	3.0	5
21	···	···	1	···	−30.0	0.3	3.0	10
22	3.6	0.04	···	···	···	0.3	3.0	10
28	2.2	0.04	···	···	···	0.3	3.0	5
29	···	···	···	···	···	0.3	3.0	5
31	···	···	···	···	···	0.15	1.5	5

Here σ_f^2, variance of $f = \log K_s$ (log: natural logarithm); σ_a^2, variance of $a = \log \alpha$; ρ_{af}, correlation coefficient between f and a; Γ, geometric mean of α [m^{-1}]; H, mean soil water tension [m]; Δx, horizontal discretization of finite elements [m]; λ_{fx}; horizontal correlation length of f[m]. For information regarding cut; see text.

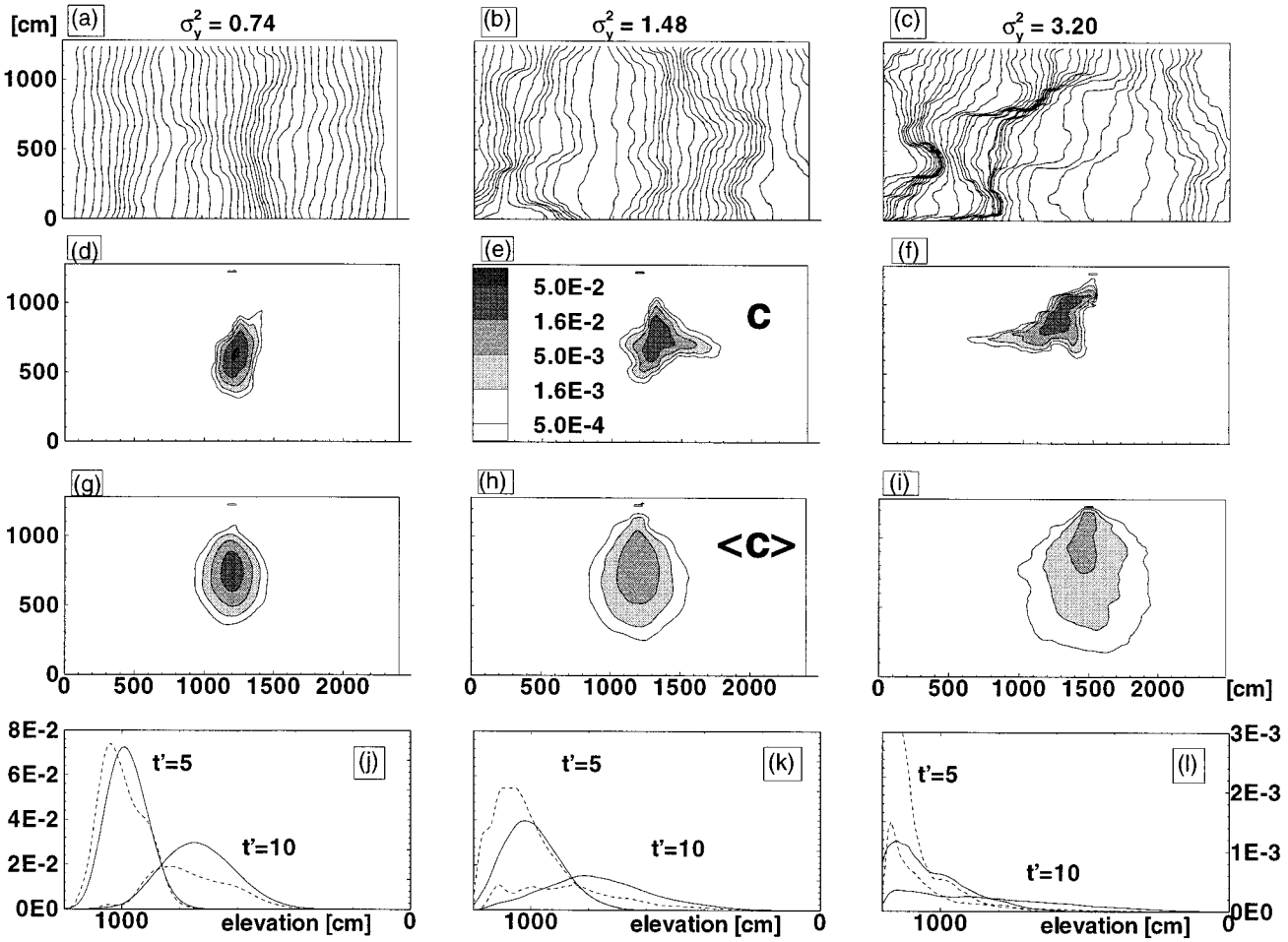

Figure 1. Examples of solute transport in three different soils with increasing variability in unsaturated hydraulic conductivity: Soil sites 29 (left column of four panels), 15 (center column), and 22 (right column). (Figures 1a–1c) Streamlines of individual realizations. (Figures 1d–1f) Respective solute concentration distributions at $t' = 10$. (Figures 1g–1i) Mean concentration distribution from 300 realizations. (Figures 1j–1*l*) Vertical profiles of concentration mean (solid line, left y axis scale) and variance (dashed line, right y axis scale) along the mean travel path at different dimensionless times t'. All horizontal and vertical distances are in centimeters.

particularly for highly variable soils. Hence 300 realizations are considered adequate for our analysis. Typically, CPU time per realization (including random field generation, flow, and transport computation) range from 5 to 15 min on an IBM RS6000/560 [see *Tripathi and Yeh*, 1993], depending primarily on σ_y^2.

Results and Discussion

General Characteristics of Solute Movement

Effects of heterogeneity on the variability in velocity and on the spatial distribution of solute concentration in unsaturated porous media are illustrated in Figure 1 for three anisotropic soils ($\nu = 6$) with distinctly different σ_y^2. In mildly heterogeneous soils, streamlines are approximately vertical (Figure 1a). As soils are more heterogeneous or as a soil dries out, streamlines tend to be clustered in preferential flow areas showing large variability over short distances. Deviations from a parallel vertical flow pattern become larger as the variability of y increases (Figures 1b and 1c), and streamlines exhibit significant lateral flow paths (Figure 1c). Relative to its entry position, the maximum observed total horizontal displacement of a streamline at the bottom of the 12-m-deep vertical section is 1 to 2 m for $\sigma_y^2 = 0.74$, on the order of 5 m for $\sigma_y^2 = 1.48$, and on the order of 10 m for $\sigma_y^2 = 3.20$. This qualitative result is consistent with the moisture-dependent anisotropy concept developed by *Yeh et al.* [1985b, c], which suggests significant lateral migration of water as soils dry out. While single realizations of streamlines as depicted in Figure 1 bear little statistical significance, they clearly illustrate why parallel stream tube models are limited in their applications when one models unsaturated solute transport from small sources.

Figures 1d–1f show actual solute concentration at $t' = 10$, which are affected by travel path variability, local dispersion, and travel velocity variability. With increasing variance of y, solute plumes assume increasingly erratic shapes; at identical dimensionless travel time t', travel distances of the plume center of mass become more variable and differ significantly from mean displacement, and the degree of lateral migration of individual solute plumes increases.

Corresponding MCS sample mean concentrations (Figures 1g–1i) exhibit more spreading and hence lower peak concentrations than observed for the actual plumes, owing to the

variability var (M_i) $(I = x, z)$ in the travel path of the plume center as the flux heterogeneity increases. In moderately to strongly heterogeneous flux the mean concentration along the vertical axis is significantly skewed (Figures 1k and 1*l*). Asymmetry in the mean concentration profile increases with σ_y^2. It is believed to be caused by the non-Gaussian velocity distribution and by significant correlation between transverse and longitudinal velocity components when the velocity is large [*Harter*, 1994]. A standard particle-tracking analysis in the velocity fields generated by simulation of soil site #3 confirmed that the skewed mean concentration distribution is not an artifact of the MMOC transport model. Only for mildly heterogeneous media, MCS simulations produce a Gaussian mean concentration distribution at all t', $5 \leq t' \leq 40$, (Figure 1g).

Sample concentration variance along the mean flow direction is significantly more skewed than the concentration mean (Figures 1j–1l). At 300 realizations it is very sensitive to outliers, particularly in highly heterogeneous soils (Figure 1*l*). Generally, the largest variances along the vertical mean flow path occur near the inflection points of the mean concentration profile if the soil is only moderately homogeneous ($\sigma_y^2 < 0.5$). In those soils the concentration variance at the plume center has a local minimum. This observation is consistent with theoretical findings [e.g., *Graham and McLaughlin*, 1989; *Neuman*, 1993]. As the flux heterogeneity increases, the concentration variance upstream of the maximum mean concentration becomes relatively larger than that downstream of the maximum mean concentration resulting in a single peak profile (Figure 1j). For very heterogeneous systems the double peak is entirely obscured due to the asymmetry of the concentration variance profile (Figure 1*l*). In single-peaked concentration variance profiles the maximum concentration variance occurs near the upstream inflection point of the mean concentration profile.

Concentration variance is a relatively poor measure of uncertainty since concentration is nonstationary. Another measure of uncertainty is concentration coefficient of variation $CV_c(\mathbf{x}, t)$

$$CV_c = \frac{\sigma_c}{\langle c \rangle} \tag{6}$$

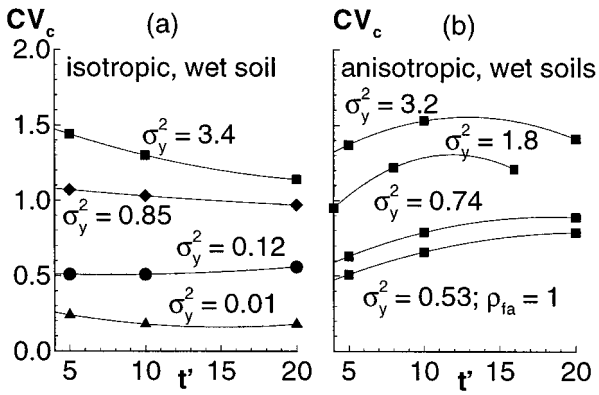

where $\langle \quad \rangle$ refers to sample averages and the evaluation is at $\mathbf{x}$ and t. Unlike concentration variance, CV_c always has a global minimum near the location of the peak mean concentration and increases with distance from the plume center [e.g., *Dagan*, 1984; *Rubin*, 1991; *Kapoor and Gelhar*, 1994]. In terms of CV_c, uncertainty about high concentrations in the center of the plume is lowest while uncertainty about the very low mean concentrations at the edges of the plume is highest. In the MCS's, the minimum CV_c is located at or below the location of mean concentration with distances between the two locations increasing as σ_y^2 increases (Table 2).

The minimum CV_c near the center of the mean plume increases with σ_y^2 (Figures 2a and 2b). At $t' \geq 5$ the minimum CV_c decreases with time or remains almost constant in wet, isotropic soils (Figure 2a) but first increases and later remains constant or decreases in wet, anisotropic soils (Figure 2b). The minimum CV_c at $t' = 5$ is higher in isotropic soils than in anisotropic soils. At later times ($t' = 10, 20$) the observed difference in CV_c for different aspect ratios decreases, and in some instances anisotropic soils will have a higher CV_c than isotropic soils of comparable textural variability. For soils of comparable σ_y^2, but different mean head (dry versus wet), temporal dynamics and magnitude of minimum CV_c are very similar. These numerical results qualitatively support the theoretical work by *Kapoor and Gelhar* [1994], who postulate that the CV_c does not increase infinitely as time becomes large. However, it should be pointed out that for most cases, the minimum CV_c is always greater than 0.5 within the time interval observed here. In many practical cases, unconditional mean concentration predictions are therefore associated with large uncertainties [*Yeh*, 1992].

Comparisons With Approximate Analytical Solutions

Spatial moments. In linear theories of macrodispersion [*Gelhar and Axness*, 1983; *Dagan*, 1984, 1988; *Neuman et al.*, 1987], the second spatial moment (moment of inertia) of the mean concentration plume is estimated analytically based on the fundamental result of turbulent diffusion [*Taylor*, 1921]